# Crystal Structure of a Thermostable Lipase from Bacillus stearothermophilus P1

**ARTICLE** *in* JOURNAL OF MOLECULAR BIOLOGY · DECEMBER 2002

Impact Factor: 4.33 · DOI: 10.1016/S0022-2836(02)01004-5 · Source: PubMed



**5 AUTHORS**, INCLUDING:

Joel D A Tyndall
University of Otago
**83** PUBLICATIONS **3,106** CITATIONS
SEE PROFILE

Linda A Fothergill-Gilmore
The University of Edinburgh
**131** PUBLICATIONS **3,422** CITATIONS
SEE PROFILE

Paul Taylor
The University of Edinburgh
**86** PUBLICATIONS **2,225** CITATIONS
SEE PROFILE

doi:10.1016/S0022-2836(02)01004-5 available online at http://www.idealibrary.com on IDEAL® J. Mol. Biol. (2002) 323, 859–869

JMB

# Crystal Structure of a Thermostable Lipase from *Bacillus stearothermophilus* P1

**Joel D. A. Tyndall[1], Supachok Sinchaikul[1,2], Linda A. Fothergill-Gilmore[1] Paul Taylor[1] and Malcolm D. Walkinshaw[1]***

[1]*Structural Biochemistry Group Institute of Cell and Molecular Biology, University of Edinburgh, Michael Swann Building, King's Buildings Mayfield Road, Edinburgh EH9 3JR, Scotland, UK*

[2]*Department of Chemistry Faculty of Science, Chiang Mai University, Chiang Mai 50200 Thailand*

**Corresponding author*

We describe the first lipase structure from a thermophilic organism. It shares less than 20% amino acid sequence identity with other lipases for which there are crystal structures, and shows significant insertions compared with the typical α/β hydrolase canonical fold. The structure contains a zinc-binding site which is unique among all lipases with known structures, and which may play a role in enhancing thermal stability. Zinc binding is mediated by two histidine and two aspartic acid residues. These residues are present in comparable positions in the sequences of certain lipases for which there is as yet no crystal structural information, such as those from *Staphylococcal* species and *Arabidopsis thaliana*. The structure of *Bacillus stearothermophilus* P1 lipase provides a template for other thermostable lipases, and offers insight into mechanisms used to enhance thermal stability which may be of commercial value in engineering lipases for industrial uses.



*Keywords:* *Bacillus stearothermophilus* P1; bacterial thermostable lipase; lipase closed conformation; metal ion stabilisation; zinc-binding site

## Introduction

Lipases (triacylglycerol acylhydrolases, EC 3.1.1.3) are present in many different organisms, and catalyse the hydrolysis of long-chain triglycerides into fatty acids and glycerol. These enzymes are of considerable commercial interest for biotechnological applications such as detergents, food production, pharmaceuticals and industrial synthesis of fine chemicals (see review by Jaeger & Reetz[1]). In particular, thermostable lipases from thermophilic bacteria have the potential to play important roles in industrial applications because they possess relatively high thermodynamic stability both at elevated temperatures and in organic solvents.[2–4]

Bacterial lipases are members of the structural superfamily of α/β hydrolases[5] whose enzymic activity results from the catalytic triad Ser-His-Asp similar to that found in serine proteinases. Generally, the serine residue occurs in the pentapeptide chain of Gly-Xaa-Ser-Xaa-Gly, except in the *Bacillus* lipases where the first glycine is replaced by an alanine. Bacterial lipases have been classified into families with the *Bacillus* lipases falling into subfamily five of family I (I.5). This family consists of lipases from Gram-positive organisms.[6]

To date, a total of nine bacterial lipase structures have been solved, four of these being true lipases; one from family I.1 (*Pseudomonas aeruginosa*, PAL[7]), and three from I.2 (*Pseudomonas glumae*, PGL,[8] *Chromobacterium viscosum*, CVL,[9] and *Pseudomonas cepacia*, PCL[10–12]). The remaining five are related lipolytic enzymes from families II (GDSL) (*Streptomyces scabies*, SsEST[13]), III (*Streptomyces exfoliatus*, SEL[14]), IV (HSL) (*Alcaligenes eutrophus*, esterase[15]), VI (*Pseudomonas flurorescens*, PFC[16]) and VII (*Bacillus subtilis*, BFAE[17]).

The active site of the majority of bacterial lipases is covered by an α-helical flexible "lid" that in the closed position maintains the catalytic triad in a hydrophobic environment isolated from aqueous solvents. The term interfacial activation[18] is used to describe the enhancement of lipase activity that occurs when the lid is triggered to open by the interaction of the enzyme with the interface of a

Present address: J. D. A. Tyndall, Institute for Molecular Bioscience, University of Queensland, Brisbane 4072, Australia.

Abbreviations used: RMSD, root-mean-square deviation; BSP, lipase from *Bacillus stearothermophilus* P1; CVL, lipase from *Chromobacterium viscosum*; PCL, lipase from *Pseudomonas cepacia*; PAL, lipase from *Pseudomonas aeruginosa*.

E-mail address of the corresponding author: m.walkinshaw@ed.ac.uk

 

**Table 1.** Data collection and phase refinement statistics

| Derivative[a] | Native | $K_2PtCl_4$ | $HgCl_2$ | EMTS[b] |
|---|---|---|---|---|
| Resolution (Å) | 2.2 | 2.4 | 2.5 | 2.5 |
| No. of observations | 211,130 | 214,389 | 79,129 | 121,289 |
| No. of independent reflections | 47,208 | 35,676 | 28,038 | 32,900 |
| $R_{merge}$[c] (%) | 10.6 | 6.3 | 7.3 | 10.9 |
| Top shell | 29.8 | 12.7 | 17.5 | 40.3 |
| Completeness (%) | 99.2 | 96.8 | 87.4 | 99.7 |
| Top shell | 91.9 | 95.5 | 76.7 | 98.3 |
| $I/\sigma I$ | 11.2 | 19.2 | 11.2 | 11.4 |
| Top shell | 4.2 | 13.6 | 4.6 | 3.1 |
| No. of sites per molecule | | 2 | 4 | 4 |

[a] Conditions.
[b] Sodium ethyl mercurithiosalicylicate.
[c] $R_{merge} = \Sigma_h\Sigma_i|I_{hi} - \langle I_h\rangle|/\Sigma_h\Sigma_i I_{hi}$.

lipid–water bilayer. Derewenda[19] describes the anatomy of the conformational changes associated with this flexible lid region using *Rhizomucor miehei* triacylglyceride lipase[18,20] as a key example. Of the bacterial lipase crystal structures released to date, PGL and CVL have both been crystallised in the closed conformation, whereas the structures of PCL and PAL have been crystallised in the open conformation both with and without bound ligands.

*Bacillus stearothermophilus* P1 lipase (BSP) occurs in the I.5 family along with two other highly thermostable enzymes. These bacterial lipases isolated from *Bacillus thermocatenulatus*[2] and *B. stearothermophilus* L1[4] have high sequence identity with BSP (~95%). All possess a complete sequence of 417 residues including a 29-residue signal sequence that is cleaved to produce the mature 388-residue lipase. The optimum activity of all three thermostable lipases lies around 65 °C and pH 8.0–9.0. Calcium-dependent stability has been demonstrated by Kim and co-workers,[21] who showed that lipase BSL1 begins to unfold at 66 °C in the presence of calcium ions, but at 58 °C in the absence of calcium.

We report here the first structure of a 43 kDa thermostable lipase isolated from *B. stearothermophilus* P1. It possesses significant differences from the known fold of the α/β hydrolase family,[22,23] and contains both a calcium ion and a zinc ion, not previously found in lipases.

## Results and Discussion

### X-ray structure determination

Lipase P1 from *B. stearothermophilus* was purified from a recombinant expression system by anion-exchange chromatography and gel filtration. Crystals were obtained by the hanging drop vapour diffusion method and data were collected as described.[24] The closest homologue lipase for which there is an X-ray structure is PCL (PDB code 4lip). However, it has only 17% amino acid sequence identity, and all attempts at using molecular replacement with this structure as a model failed. The structure was finally determined by multiple isomorphous replacement (MIR) using three heavy atom derivatives (with anomalous scattering). The data collection and structure refinement statistics are given in Table 1.

The quality of the electron density map was excellent and allowed unambiguous tracing of all amino acid residues in the sequence (see e.g. Figure 1).

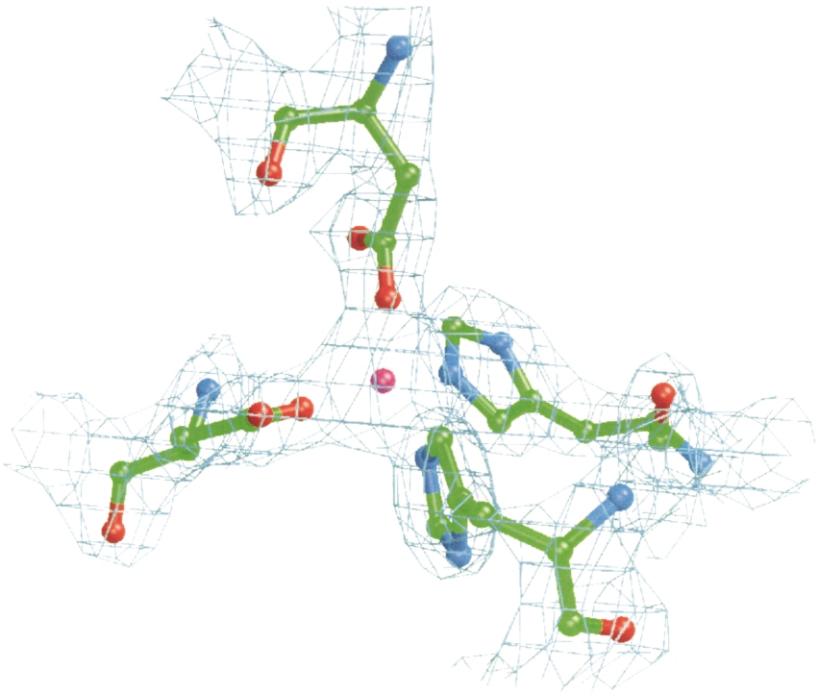

**Figure 1**. Coordination environment around the $Zn^{2+}$. The zinc (magenta sphere) is coordinated tetrahedrally by Asp61, His81, His87 and Asp238 with zinc ligand distances of 2.12 Å, 1.98 Å, 2.13 Å and 1.96 Å, respectively. The diagram was generated with Bobscript.[41]

**Table 2.** Refinement statistics

| | |
|---|---|
| Resolution range (Å) | 40.0–2.20 |
| *a* (Å) | 118.5 |
| *b* (Å) | 81.2 |
| *c* (Å) | 99.8 |
| β (deg.) | 96.3 |
| % Solvent | 55.12 |
| $V_m$ (Å$^3$ Da$^{-1}$) | 2.76 |
| $R_{factor}$[a] (%) | 16.6 |
| $R_{free}$[b] (%) | 21.7 |
| Number of residues per BSP molecule | 388 |
| Number of water molecules | 347 |
| Number of calcium ions per BSP molecule | 1 |
| Number of zinc ions per BSP molecule | 1 |
| RMSD | |
| Bond lengths (Å) | 0.218 |
| Bond angles (deg.) | 1.256 |
| Ramachandran plot | |
| Residues in most-favoured region (%) | 91.7 |
| Residues in additional allowed regions (%) | 7.9 |
| Residues in disallowed regions (%) | 0.5 |

| Average *B* factors (Å$^2$) | Molecule A | Molecule B | Overall |
|---|---|---|---|
| Main-chain atoms | 26.8 | 24.3 | 25.5 |
| Side-chain atoms | 31.2 | 28.6 | 30.2[c] |
| All atoms | 29.0 | 26.4 | 28.0 |

[a] $R_{factor} = \Sigma_h||F_{obs}| - |F_{calc}||/\Sigma|F_{obs}|$, where $F_{obs}$ and $F_{calc}$ are the observed and calculated structure factor amplitudes, respectively.
[b] $R_{free}$ is calculated with 5% of the diffraction data, which were not used during the refinement.
[c] Side-chains + 347 water molecules.

The structure has been refined to 2.2 Å with an $R_{factor}$ of 16.6% and an $R_{free}$ of 21.7% (Table 2). There are two independent molecules per asymmetric unit, each comprising 388 residues, together with 1 $Ca^{2+}$ and 1 $Zn^{2+}$ per molecule. X-ray fluorescence was carried out to confirm the identity of the zinc ion. A clear signal was obtained at 9.769 keV (Figure 2), which corresponds to the absorption edge of zinc that has a theoretical value of 9.659 keV. No signal was observed around the theoretical absorption edge of copper at 8.98 keV.

## Description of overall protein fold

Each BSP molecule has a generally globular shape with approximate dimensions of 40 Å × 50 Å × 65 Å (Figure 3). The α/β hydrolase fold of BSP is similar to that seen for other lipases, though there are a number of unique structural features. The core structure consists of a seven-stranded parallel sheet that is surrounded by alpha helices 1 and 13 on one side, and alpha helices 2, 4, 5, 9, 10, 11 and 12 on the other side.

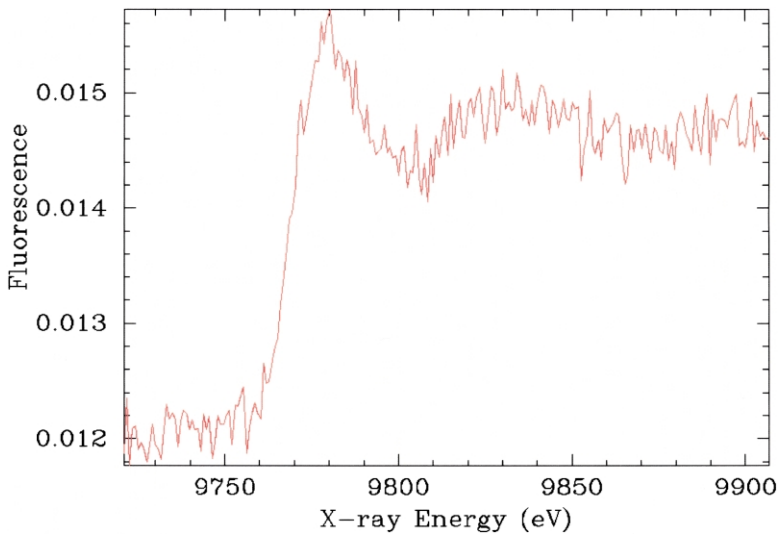


**Figure 2**. Fluorescence signal from a single crystal of BSP showing the presence of zinc. Synchrotron radiation from SLS station 9.5 was used to provide a monochromatic X-ray beam which was scanned over the energy range 9.72 keV to 9.9 keV.

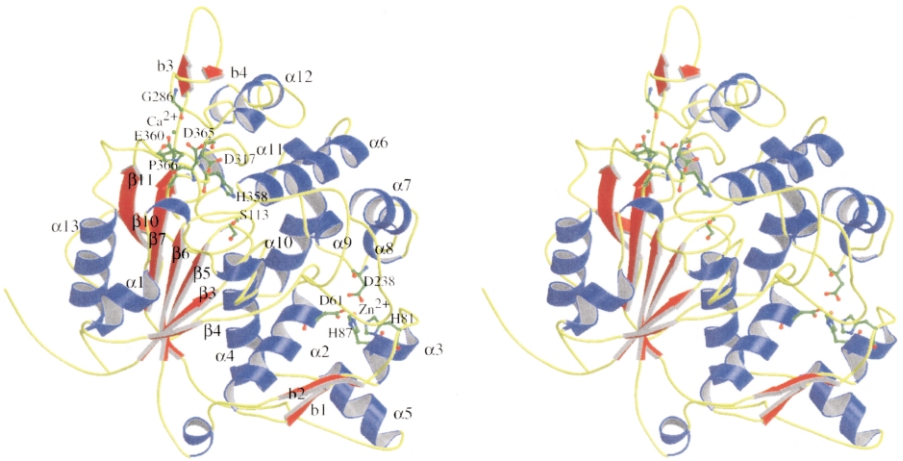


**Figure 3**. Structure of *B. stearothermophilus* P1 lipase. Stereo representation of the secondary structure as determined by DSSP[42] and generated using MOLSCRIPT and Raster 3D.[43] Alpha helices, beta strands and loops are shown in blue, red and yellow, respectively. The labelled residues, from left to right, are the calcium-binding residues, Glu360, Gly286, Pro366 and Asp365 with calcium in green; the catalytic triad, Asp317, His358 and Ser311, and the zinc-binding residues, Asp61, His87, Asp238 and His81 with zinc in orange.

The secondary structure topology of BSP is compared to that of the canonical α/β hydrolase fold in Figure 4(a) and (b), respectively. BSP lacks the N-terminal antiparallel beta sheet of the canonical fold (strands β1 and β2, Figure 4(b)), which is not uncommon for bacterial lipases. Helix α6 and the adjacent loop region (Figure 3; see also Figures 6 and 7) make up the lid which, in its closed position, isolates the substrate-binding cleft from solvent.

The most significant deviation from the recognised canonical fold is the large insertion (approximately 25 residues) at helix αB (canonical fold, Figure 4(b)), which contains two of the four $Zn^{2+}$-binding residues (His81 and His87). The peptide chain then returns to the canonical fold of helix αB as a $3_{10}$ helix followed by strand β5. Another deviation from the general fold exists at helix α4 and strand β6, where helix α5 is inserted with a loop region on either side (Figure 4(a)). This is adjacent to the $Zn^{2+}$-binding region mentioned above, and is involved in hydrogen-bonding interactions between the two areas.

Both molecules in the asymmetric unit are very similar, and superimposition of alpha carbon atoms gives a root-mean-squared deviation (RMSD) of 0.36 Å. Superimposition of all non-hydrogen atoms gives an RMSD value of 0.77 Å. The Ramachandran plot shows that 91.7% (607) of residues lie in the most-favoured region, with 7.9% (52) of residues in the additional allowed region (Figure 5, Table 2).

The catalytic serine residues (Ser113) of both the molecules lie in the generously allowed region. This is a typical conformation for the "nucleophilic elbow", which is positioned in a tightly constrained beta turn type structure between a beta strand and an alpha helix.[8,22,25] Val203 residues of both molecules are found in the disallowed region. There is clearly defined electron density for this residue that is positioned on a long loop between helix α6 (the flexible lid) and helix α7 (see Figure 3). The *B* factors of the backbone atoms are 31.8 and 29.1 Å$^2$ in the two BSP molecules, which are slightly higher than the average discussed below (see Table 2). The isopropyl side-chain is part of a larger hydrophobic cleft protected from solvent by the closed lid, and appears to be distorted by the hydrophobic effect.

Phe25 of molecule A also lies in the generously allowed region ($\phi = 16°/\psi = 93°$). This is due to the close proximity of the same residue on a molecule related by twofold crystallographic symmetry. The average *B* factor for the side-chain atoms of Phe25 is 44.2 Å$^2$, which is significantly higher than the overall averages shown in Table 2. Another residue, Asp310, is somewhat distorted and is involved in multiple hydrogen-bonding interactions with both Thr74 and Thr93, which are situated in the zinc-binding region of a symmetry-related molecule.

Prior to the determination of the crystal structure of BSP reported here, a three-dimensional model of BSP was proposed.[26] The model was based on secondary structure predictions and secondary structure-driven multiple sequence alignment with two bacterial lipases of known crystal structure, PGL and PCL. Comparison of the model with the determined structure reported here shows the model to be correct in most aspects, although the novel zinc-binding domain was not identified.

The sequence of BSP shows high conservation when compared to the sequences of the thermostable lipases from *B. thermocatenulatus*[27] and *B. stearothermophilus* L1 for which a preliminary X-ray analysis has been reported.[4,28] It is anticipated that all the structural features of BSP described here will apply to the structures of these two lipases.

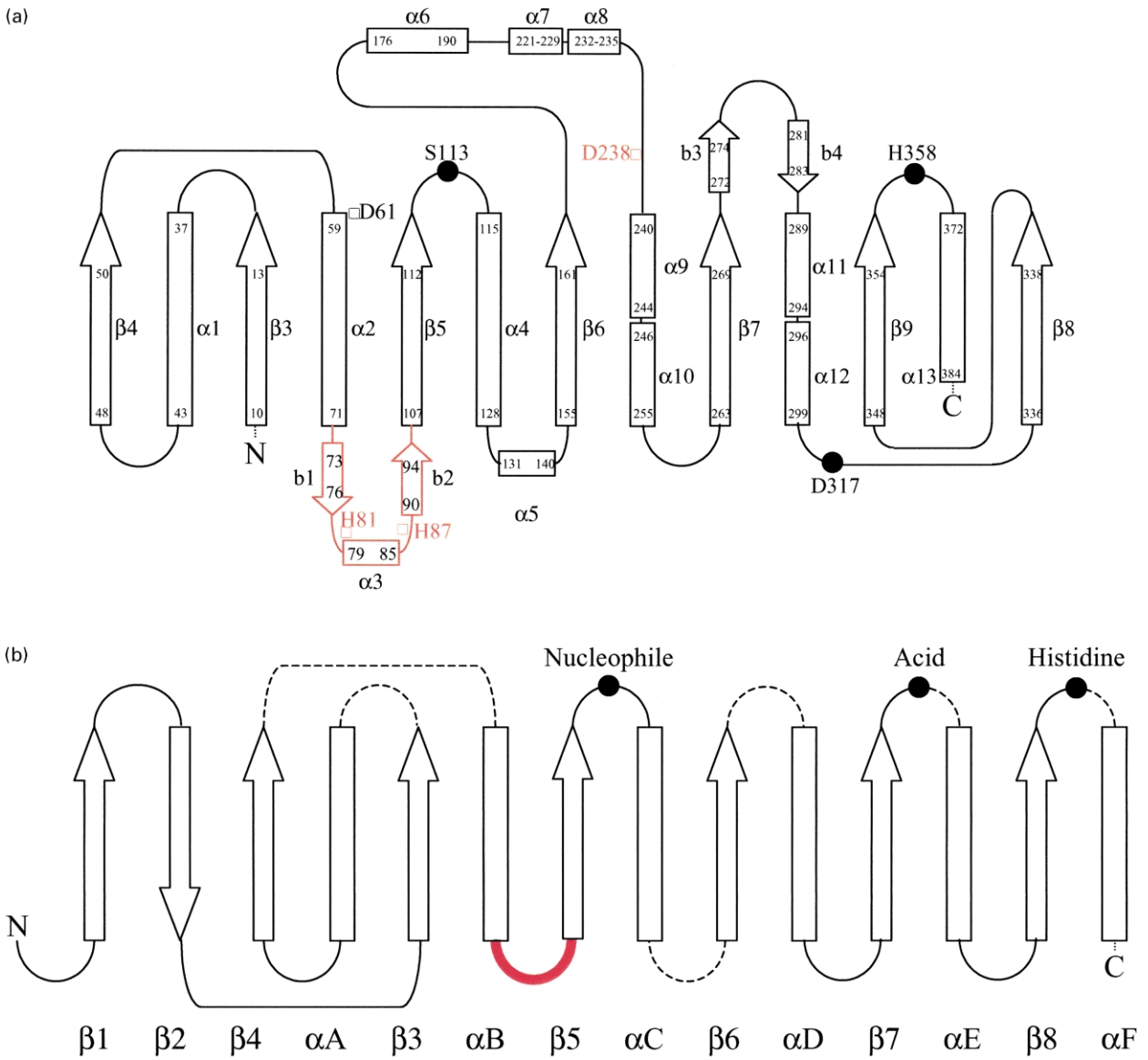


**Figure 4**. Comparison of the secondary structure of BSP with the canonical lipase fold. (a) Secondary structure topology of BSP showing the general α/β hydrolase fold including the catalytic triad and the zinc-binding structural elements and residues indicated in black and red, respectively. Alpha helices and beta strands are represented by rectangles and arrows, respectively. New structural elements, strand b1, helix α3 and strand b2 are shown in red. (b) Secondary structure topology diagram of the canonical α/β hydrolase fold. Broken lines indicate possible sites of insertions. The heavy line depicts the position of the new deviation from the known fold.

## Description of the active site

The catalytic triad consists of Ser113, His358 and Asp317 as described by Sinchaikul and co-workers[26] (see Figure 3). The catalytic serine is situated on the nucleophilic elbow between strand β5 and helix α4 deep within the core structure. In *Bacillus* lipases the serine is embedded within the Ala-Xaa-Ser-Xaa-Gly consensus sequence (where Xaa represents His and Gln, respectively). The active site is isolated from solvent by a flexible alpha helical lid (helix α6) similar to that found in the structures of CVL and PGL. The active site is also bounded by helix α11 and α12 (separated only by Cys295). Helix α6 would most likely be involved in a conformational change that allows the substrate access to the active site. The nature of these enzymes dictates that the active site is quite hydrophobic. Within the small active site cavity there is only one water molecule that makes hydrogen-bonding interactions with Thr17 and Tyr29 on the base of the cavity.

On closer investigation, the active site and the interface between the proposed active site floor and the flexible lid region consist predominantly of aromatic and other hydrophobic residues (Figure 6). They include Phe16 (that immediately follows strand β3), Trp19, Met24, Tyr29, Pro55 and Leu56. A $3_{10}$ helical turn positions Leu170 towards the active site, and this is followed by Phe176,

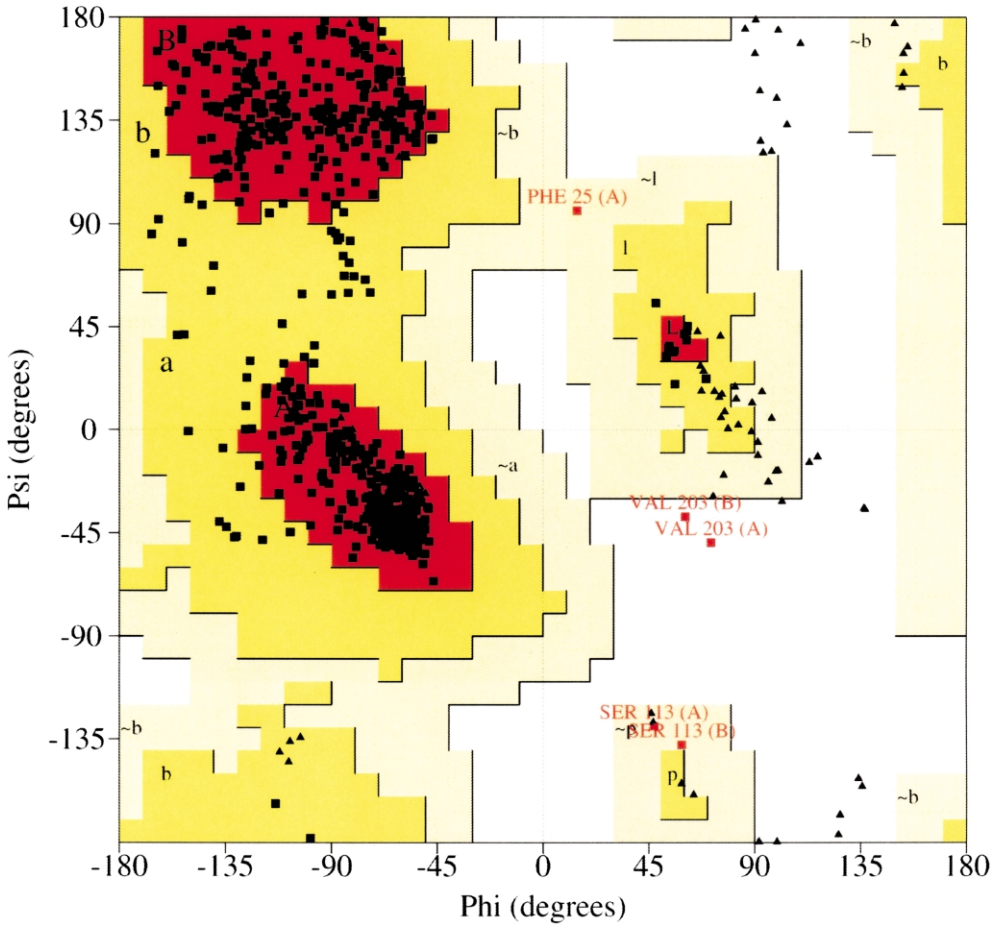


**Figure 5**. Ramachandran plot of the two molecules of BSP in the asymmetric unit. Glycine residues are shown as triangles. Core regions are shaded red, with additional allowed and generously allowed zones in progressively lighter shades of yellow. Disallowed zones are unshaded. See the text for description of labelled residues.

Phe180, Phe181, Leu183, Val187 and Leu188, which make up the amphipathic helix α6 (Figure 3). Only one of a few non-hydrophobic residues within the active site, Gln184, stands out. The side-chain amide nitrogen of this residue forms a hydrogen bond with the main-chain carbonyl oxygen of Phe16, possibly forming an anchor to keep the lid from opening. Further enclosed with the lid region are Tyr204 and Phe206, followed by Phe221, Phe225, Leu228 and Trp234 of helices α7 and α8. The apparently more rigid side is bounded by Phe290 and Leu299 of helices α11 and α12, respectively. Ile319 (that lies above the catalytic Asp317 and His358) and Ile362 make up the

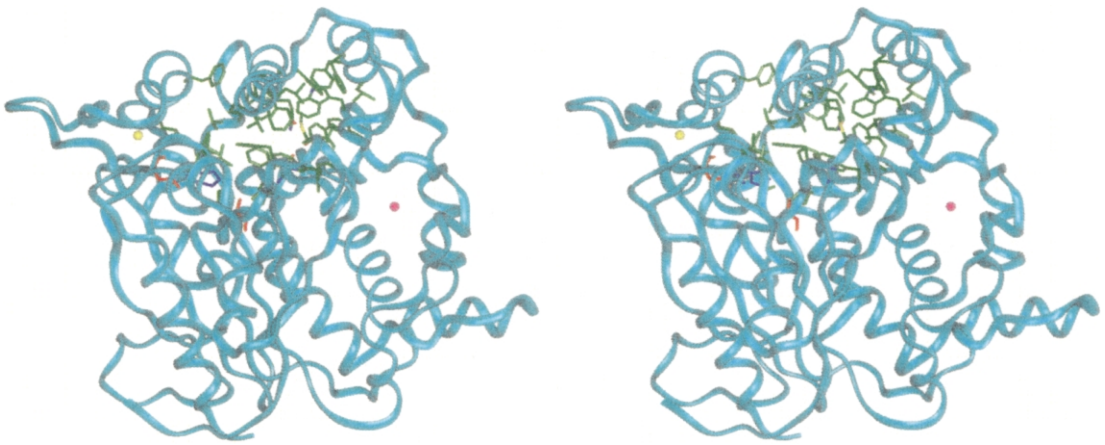

**Figure 6**. Stereo view of BSP with the aromatic and hydrophobic residues of the lid region coloured green. The catalytic triad residues (Ser113, His358 and Asp317) are shown from left to right in red, blue and red. The calcium ion is yellow, and the zinc is magenta.

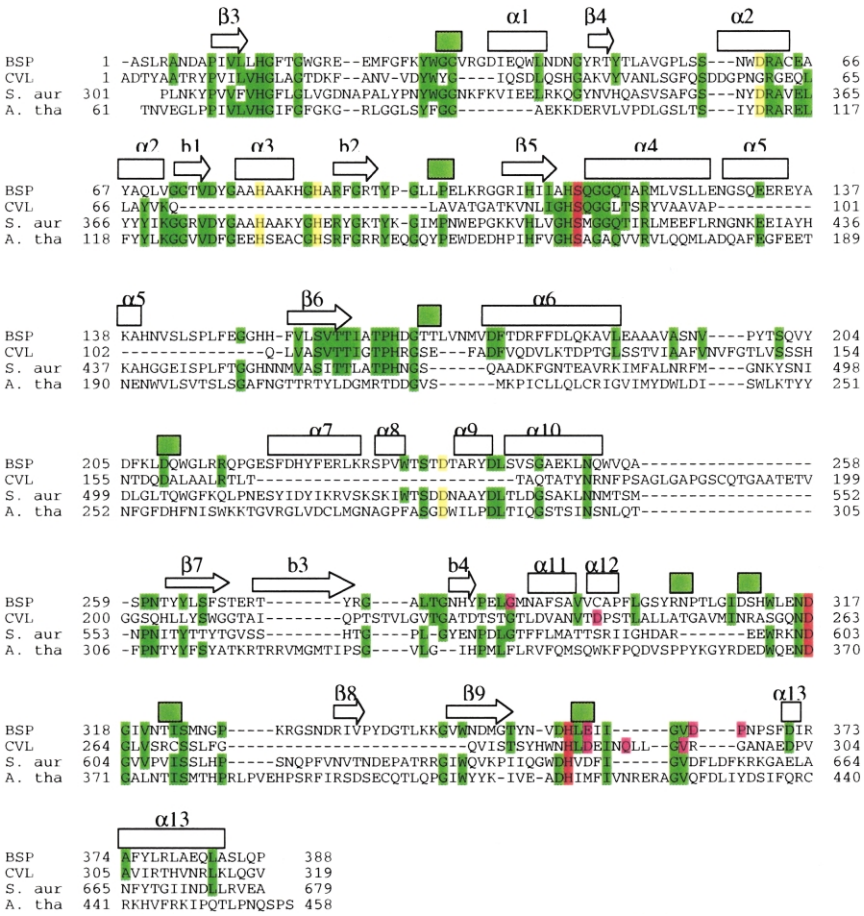

**Figure 7**. Sequence alignment of BSP with CVL and lipases from *S. aureus* and *A. thaliana*. The secondary structure of BSP is represented above the sequences as white barrels and arrows for alpha helices and beta strands, respectively. Grey-shaded barrels represent $3_{10}$ helices. The green-shaded residues indicate sequence identity. The residues of the catalytic triad are shaded red. Residues involved in zinc binding are shaded yellow, and those in calcium binding are shaded pink.

remainder of the hydrophobic residues within the cavity.

Inspection of a surface representation of BSP shows what appears to be a channel leading towards the active site. It is clear that this is a portion of the substrate-binding cleft and is surrounded by the hydrophobic residues Phe27, Leu33, Val187, Ala190, Leu359 and Val364. The latter two residues are adjacent to the catalytic histidine and one of the calcium-binding residues. A comparison of BSP with PAL in complex with a triacylglycerol analogue shows that the *sn*-2 chain of this inhibitor does indeed bind in a similar channel in PAL. This suggests that BSP would bind a triacylglycerol substrate in a similar manner following the opening of the flexible lid.

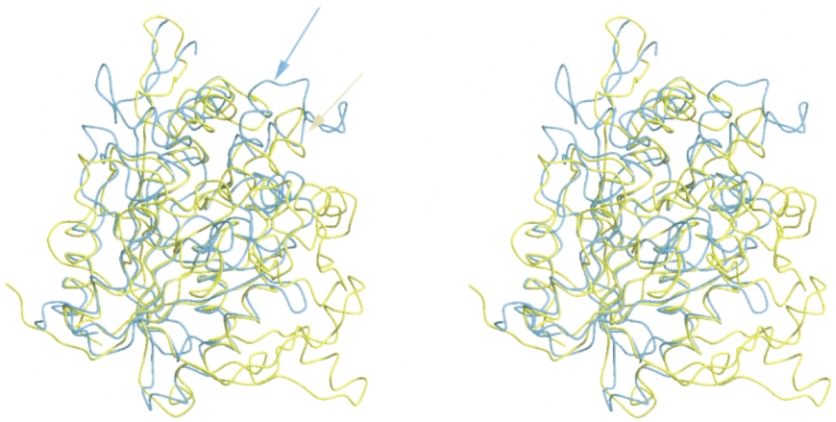

**Figure 8**. Superimposition of CVL on BSP. The structures are in a similar orientation to Figure 3. Conserved secondary structural elements were superimposed consisting of N, alpha C and C atoms of 88 residues from both proteins. The backbone atoms of residues 8–15, 40–53, 62–70, 108–125, 157–169, 248–254, 262–268, 349–353 and 373–379 of BSP (yellow) were superimposed upon residues 9–16, 36–49, 61–69, 82–99, 106–118, 171–177, 204–210, 275–279 and 304–310 of CVL (blue). These residues correspond to the majority of strand β3, a portion of helix α1 and strand β4, helix α2, strand β5 and helix α4 including the nucleophilic elbow, strand β6, helix α10, strand β7, strand β9 and helix α13 of BSP (see Figure 4 for further details). The flexible lids in both proteins are indicated by an arrow.

### Comparison to the mesostable lipase CVL

The sequence of BSP is compared to that of CVL, to a lipase from *Staphylococcus aureus* and to a putative lipase from *Arabidopsis thaliana* in Figure 7. The secondary structural elements of BSP are shown, as well as residues implicated in catalysis and metal ion binding. The alignment shows the structurally related alignment associated with CVL. It would appear that the related lipases of *Staphylococcus* spp. and *A. thaliana* are likely to have a very similar overall fold to BSP. In addition, they are likely to bind a zinc ion, given the high degree of sequence identity in the region corresponding to the known zinc-binding site of BSP. However, the calcium-binding residues are not similar between the known structures of BSP and CVL.

A superposition of the X-ray structures of BSP and CVL is shown in Figure 8. CVL is in the unligated form with the flexible lid in the closed conformation, unlike PAL that tends to remain in a much more open structure. Residues of CVL that were superimposed on those of BSP correspond to strand β3, a portion of helix α1 and strand β4; helix α2, strand β5 and helix α4 including the nucleophilic elbow; strand β6, helix α10, strand β7, brand β9 and helix α13 (Figure 4). The two structures have an RMSD value of 0.84 Å. The core beta sheet is well conserved, as is helix α4 that follows the nucleophilic elbow and is a well--conserved feature of the α/β hydrolase structures.[22] Helices α1 and α13 on one side, and helix α2 on the other side are also relatively well-conserved. Helices α11 and α12, at the left of the active site lid in Figure 3, correspond to helix 9 of the CVL structure. Helix α10 at the rear of the structure in Figure 3 is in a similar position to helix α7 of CVL.

This is where the similarities cease. As mentioned below, there is an additional zinc-binding domain adjacent to helix α2 (Figure 4(a)). Moreover, there are differences associated with the lid region. Helix α6 of BSP gives the appearance of a more tightly bound lid (Figure 8), although it is broadly similar to helix α6 of CVL (or helix B of the canonical fold in Figure 4(b)). There is a further significant deviation following helix α6 that corresponds to an insertion of approximately 50 residues (see Figures 7 and 8). This insertion consists of a large loop followed by helices α7 and α8 (broken by two residues, Arg-Ser) and helix α9. Helix α10 returns to the general fold, and corresponds to helix 7 of CVL (helix D of the canonical fold). The insertion may allow for a far greater range of movement of the lid region, and is also potentially associated with the specificity of the enzyme.

### Metal-binding sites

Helix α3 and the antiparallel beta sheet (strands b1 and b2) form a zinc-binding domain that may help to stabilise the enzyme. This feature is novel in that it is the first lipase structure found to contain a $Zn^{2+}$ as well as a $Ca^{2+}$. Furthermore, the insertion of this domain between helix αB and strand β5 has not, until now, been seen within the α/β hydrolase canonical fold (Figure 4(b)).[5]

The $Ca^{2+}$ is coordinated in an octahedral environment *via* Gly286 O, Glu360 $O^{\varepsilon 2}$, Asp365 $O^{\delta 1}$, Pro366 O and two water molecules. The second coordinating water molecule can only be seen in one of the two molecules in the asymmetric unit. All calcium–ligand distances are approximately 2.4 Å, which is in accordance with reported values.[29]

The $Zn^{2+}$ is coordinated in a tetrahedral environment by two histidine $N^{\varepsilon 2}$ atoms (His81 and His87) located in helix α3, and two aspartate $O^{\delta}$ atoms (Asp61 and Asp238) (Figure 1). All zinc–ligand distances are between 2.0 Å and 2.2 Å, which are as expected for zinc.[29] The $Zn^{2+}$ is approximately 19 Å away from the catalytic serine residue, and is thus unlikely to participate in catalysis. Instead, it could be suggested that it plays a role in conferring enhanced stability. The zinc-binding motif consists of two histidine and two aspartic acid residues. These residues are present in comparable positions in the sequences of certain lipases for which there is as yet no crystal structural information, such as those from *Staphylococcal* species and *A. thaliana* (Figure 7). The latter two organisms are mesophilic, and it will be of interest to ascertain whether their lipases show unusually enhanced thermostability.

### Factors that contribute to thermostability

All proteins exist in a dynamic equilibrium between a native-folded state and a partially unfolded state. Occasionally proteins in the partially unfolded state may undergo an irreversible process to an inactive denatured form. A thermostable protein is one for which the equilibrium lies in favour of the native-folded state at elevated temperatures (see reviews by Jaenicke & Boehm[30] and Vieille & Zeikus[31]). In general, thermostable proteins exhibit a relative lack of flexibility and thereby have a tendency to remain in the native-folded state. There are a number of different strategies by which proteins may achieve greater rigidity, each of which typically makes only a modest energetic contribution to stabilisation. Stabilising factors include: increase in surface charge networks, increase in hydrogen bonds, increase in helix-forming residues, stabilisation of helix dipoles, more and longer beta strands, fewer residues in loops, more proline residues and fewer glycine residues, reduced surface area and volume, fewer labile residues (e.g. Asn, Gln, Met, Cys), more disulphide bonds and stabilisation by ligands such as metals. Most thermostable proteins possess some, but not all of these properties.

BSP provides a possible example of ligand stabilisation, because uniquely among lipases it possesses a zinc-binding domain in addition to

the calcium binding generally found in bacterial lipases. Other examples of thermostable and hyperthermostable enzymes that contain additional metal ions not found in their mesostable analogues include proteinases in the subtilisin superfamily[32,33] and ferredoxin.[34] The latter protein from the thermophile *Sulfolobus* possesses an additional 40-residue N-terminal domain containing a zinc ion not found in mesostable homologues, but conserved in other thermoacidophiles. In addition, certain proteins contain $Zn^{2+}$ that play a purely structural role, with an obvious example being zinc fingers found in DNA-binding proteins. An important class of proteinases, the MMPs, contain a catalytic $Zn^{2+}$ as well as structural $Ca^{2+}$ and $Zn^{2+}$. It is believed that these metal ions keep the structural elements together within the catalytic domain, thus contributing to its stability.[35] The structure of aspartate transcarbamolyase[36] shows the $Zn^{2+}$ playing a crucial structural role in linking the allosteric domain to the catalytic polypeptide.

BSP possesses several other stabilising factors, and these are indicated in Table 3 in comparison with lipases CVL, PCL and PAL for which there are known crystal structures. These three lipases are all from mesophilic bacteria, and it is reasonable to assume that they do not posses unusual thermal properties. It appears that BSP (and PAL) have significantly more salt bridges, helical residues, and proline residues. Most of the 23 residues of BSP that form salt bridges occur in pairwise interactions, and are not involved in extended charged networks. In addition, BSP has an unusually high proportion of aromatic residues. However, other potential stabilising factors, such as helix dipole stabilisation or reduced glycine residues and labile residues, are not particularly different from the mesostable lipases. There is no single mechanism responsible for the stability of thermostable enzymes, but rather a combination of numerous contributing factors. A possible factor in the stability of this thermostable enzyme is the presence of the additional metal ion not seen before in this class of lipases.

The structure of the thermostable lipase BSP thus provides insight into ways in which enhanced thermal stability might be engineered into this class of enzymes. It also provides a basis for detailed structural descriptions of other thermostable lipases, such as those from *B. thermocatenulatus* and *B. stearothermophilus* L1.

**Table 3.** Factors which may contribute to protein stability

| Factor | BSP | CVL | PCL | PAL |
|---|---|---|---|---|
| Salt bridges/100 residues | 3.09 | 2.19 | 1.25 | 3.15 |
| % Strand residues | 13.4 | 16.0 | 13.4 | 12.3 |
| % Helix residues | 47.4 | 29.0 | 40.9 | 46.7 |
| Dipole stabilisations (N-caps) | 4 | 3 | 4 | 3 |
| % Pro residues | 4.6 | 3.1 | 4.1 | 4.6 |
| % Gly residues | 9.8 | 8.8 | 11.3 | 10.9 |
| % Aromatic residues | 11.6 | 6.6 | 7.5 | 8.1 |
| % Labile residues (N, Q, M, C) | 10.6 | 11.0 | 11.3 | 11.2 |
| Disulphide bonds | 0 | 1 | 1 | 1 |
| Molecular volume (Å$^3$)/residue | 131 | 122 | 121 | 123 |

## Materials and Methods

### Purification and characterisation

The gene-encoding BSP was isolated from *B. stearothermophilus* P1 that had been collected from a hot spring in Chiang Mai, Thailand. The enzyme was over-expressed in *E. coli*, and purified as described previously.[24]

### Crystallisation and data collection

BSP was crystallised from ammonium sulphate and Hepes buffer by the hanging drop, vapour diffusion method as described.[24] The lipase crystallised in the space group *C*2 with unit cell dimensions of $a = 118.5$ Å, $b = 81.2$ Å, $c = 99.8$ Å, $\alpha = 90°$, $\beta = 96.3°$ and $\gamma = 90°$. This gives a Matthews coefficient of 2.76 Å$^3$ Da$^{-1}$ assuming two molecules in the asymmetric unit. Native (2.2 Å) and derivative data were collected at the synchrotron facility in Daresbury ($\lambda = 1.2$ Å), with a MAR CCD and using cryo conditions. The data were integrated and reduced using DENZO and SCALEPACK.[37]

### Heavy atom derivatives

The structure of BSP was determined using MIR techniques. Crystals of BSP were soaked in heavy atom derivative solutions (Table 1) for approximately 30 minutes prior to freezing in liquid nitrogen. The soaking solutions consisted of 10 mM heavy atom derivatives, 22% saturated ammonium sulphate, Hepes buffer (pH 6.8–7.0) and 25% (v/v) glycerol.

The four sets of data were merged using CCP4 suite version 4.1. The program SOLVE†,[38] was used to solve and refine the heavy atom parameters and generate the initial phases. ARP warp,[39] was used for phase improvement and automated structure solution. DM was used for solvent flattening. WHAT_IF and WHATCHECK,[40] were used to check the quality of the structure.

### Determination of metal ion

An X-ray fluorescence scan of a single native crystal was carried out using the tuneable X-ray source at station 9.5 at the SRS, Daresbury. A single crystal was washed in freezing solution comprising well solution made up to 25% glycerol. The crystal was mounted in a cryoloop and flash frozen in liquid nitrogen. The input X-ray energy was scanned over regions corresponding to the *k*-absorption edges for copper (8.978 keV) and zinc (9.658 keV).

### Protein Data Bank accession numbers

The atomic coordinates and structure factors have been deposited with the Brookhaven Protein Data Bank as entry 1JI3.

† http://www.solve.lanl.gov/

## Acknowledgements

This research was supported by the Royal Academy of Engineering (RAE), Thailand Research Fund (TRF) and Edinburgh Protein Interaction Centre (EPIC). We are grateful to staff at the Synchrotron Radiation Source (SRS) at Daresbury.

## References

1. Jaeger, K.-E. & Reetz, M. T. (1998). Microbial lipases form versatile tools for biotechnology. *Trends Biotechnol.* **16**, 396–403.
2. Schmidt-Dannert, C., Rua, M., Atomi, H. & Schmid, R. D. (1996). Thermoalkalophilic lipase of *Bacillus thermocatenulatus*. I. Molecular cloning, nucleotide sequence, purification and some properties. *Biochim. Biophys. Acta*, **1301**, 105–114.
3. Schmidt-Dannert, C., Rua, M., Wahl, S. & Schmid, R. D. (1997). *Bacillus thermocatenulatus* lipase: a thermoalkalophilic lipase with interesting properties. *Biochem. Soc. Trans.* **25**, 178–182.
4. Kim, H.-K., Park, S.-Y., Lee, J.-K. & Oh, T.-K. (1998). Gene cloning and characterization of thermostable lipase from *Bacillus stearothermophilus* L1. *Biosci. Biotechnol. Biochem.* **62**, 66–71.
5. Ollis, D. L., Cheah, E., Cygler, M., Dijkstra, B., Frolow, F., Franken, S. M. *et al.* (1992). The alpha/beta hydrolase fold. *Protein Eng.* **5**, 197–211.
6. Arpigny, J. L. & Jaeger, K. E. (1999). Bacterial lipolytic enzymes: classification and properties. *Biochem. J.* **343**, 177–183.
7. Nardini, M., Lang, D. A., Jaeger, K. E. & Dijkstra, B. W. (2000). Crystal structure of *Pseudomonas aeruginosa* lipase in the open conformation. The prototype for family I.1 of bacterial lipases. *J. Biol. Chem.* **275**, 31219–31225.
8. Noble, M. E., Cleasby, A., Johnson, L. N., Egmond, M. R. & Frenken, L. G. (1993). The crystal structure of triacylglycerol lipase from *Pseudomonas glumae* reveals a partially redundant catalytic aspartate. *FEBS Letters*, **331**, 123–128.
9. Lang, D., Hofmann, B., Haalck, L., Hecht, H. J., Spener, F., Schmid, R. D. & Schomburg, D. (1996). Crystal structure of a bacterial lipase from *Chromobacterium viscosum* ATCC 6918 refined at 1.6 Å resolution. *J. Mol. Biol.* **259**, 704–717.
10. Lang, D. A., Mannesse, M. L., de Haas, G. H., Verheij, H. M. & Dijkstraand, B. W. (1998). Structural basis of the chiral selectivity of *Pseudomonas cepacia* lipase. *Eur. J. Biochem.* **254**, 333–340.
11. Kim, K. K., Song, H. K., Shin, D. H., Hwang, K. Y. & Suh, S. W. (1997). The crystal structure of a triacylglycerol lipase from *Pseudomonas cepacia* reveals a highly open conformation in the absence of a bound inhibitor. *Structure*, **5**, 173–185.
12. Schrag, J. D., Li, Y., Cygler, M., Lang, D., Burgdorf, T., Hecht, H. J. *et al.* (1997). The open conformation of a *Pseudomonas lipase*. *Structure*, **5**, 187–202.
13. Wei, Y., Schottel, J. L., Derewenda, U., Swenson, L., Patkar, S. & Derewenda, Z. S. (1995). A novel variant of the catalytic triad in the *Streptomyces scabies* esterase. *Nature Struct. Biol.* **2**, 218–223.
14. Wei, Y., Swenson, L., Castro, C., Derewenda, U., Minor, W., Arai, H. *et al.* (1998). Structure of a microbial homologue of mammalian platelet-activating factor acetylhydrolases: *Streptomyces exfoliatus* lipase at 1.9 Å resolution. *Structure*, **6**, 511–519.
15. Bourne, P. C., Isupov, M. N. & Littlechild, J. A. (2000). The atomic-resolution structure of a novel bacterial esterase. *Struct. Fold. Des.* **8**, 143–151.
16. Kim, K. K., Song, H. K., Shin, D. H., Hwang, K. Y., Choe, S., Yoo, O. J. & Suh, S. W. (1997). Crystal structure of carboxylesterase from *Pseudomonas fluorescens*, an alpha/beta hydrolase with broad substrate specificity. *Structure*, **5**, 1571–1584.
17. Wei, Y., Contreras, J. A., Sheffield, P., Osterlund, T., Derewenda, U., Kneusel, R. E. *et al.* (1999). Crystal structure of brefeldin A esterase, a bacterial homolog of the mammalian hormone-sensitive lipase. *Nature Struct. Biol.* **6**, 340–345.
18. Brzozowski, A. M., Derewenda, U., Derewenda, Z. S., Dodson, G. G., Lawson, D. M., Turkenburg, J. P. *et al.* (1991). A model for interfacial activation in lipases from the structure of a fungal lipase–inhibitor complex. *Nature*, **351**, 491–494.
19. Derewenda, Z. S. (1994). Structure and function of lipases. *Advan. Protein Chem.* **45**, 1–52.
20. Derewenda, U., Brzozowski, A. M., Lawson, D. M. & Derewenda, Z. S. (1992). Catalysis at the interface: the anatomy of a conformational change in a triglyceride lipase. *Biochemistry*, **31**, 1532–1541.
21. Kim, M.-H., Kim, H.-K., Lee, J.-K., Park, S.-Y. & Oh, T.-K. (2000). Thermostable lipase of *Bacillus stearothermophilus*: high-level production, purification, and calcium-dependent thermostability. *Biosci. Biotechnol. Biochem.* **64**, 280–286.
22. Heikinheimo, P., Goldman, A., Jeffries, C. & Ollis, D. L. (1999). Of barn owls and bankers: a lush variety of alpha/beta hydrolases. *Struct. Fold. Des.* **7**, R141–R146.
23. Nardini, M. & Dijkstra, B. W. (1999). Alpha/beta hydrolase fold enzymes: the family keeps growing. *Curr. Opin. Struct. Biol.* **9**, 732–737.
24. Sinchaikul, S., Tyndall, J. D. A., Fothergill-Gilmore, L. A., Taylor, P., Phutrakul, S., Chen, S.-T. & Walkinshaw, M. D. (2002). Expression, purification, crystallization and preliminary crystallographic analysis of a thermostable lipase from *Bacillus stearothermophilus* P1. *Acta Crystallog. sect. D*, **58**, 182–185.
25. Derewenda, Z. S. & Sharp, A. M. (1993). News from the interface: the molecular structures of triacylglyceride lipases. *Trends Biochem. Sci.* **18**, 20–25.
26. Sinchaikul, S., Sookkheo, B., Phutrakul, S., Wu, Y. T., Pab, F. M. & Chen, S. T. (2001). Structural modeling and characterization of a thermostable lipase from *Bacillus stearothermophilus* P1. *Biochem. Biophys. Res. Commun.* **283**, 868–875.
27. Schmidt-Dannert, C., Rua, M., Atomi, H. & Schmid, R. D. (1996). Thermoalkalophilic lipase of *Bacillus thermocatenulatus*. I. Molecular cloning, nucleotide sequence, purification and some properties. *Biochim. Biophys. Acta*, **1301**, 105–114.
28. Jeong, S.-T., Kim, H.-K., Kim, S.-J., Pan, J.-G., Oh, T.-K. & Ryu, S.-E. (2001). Crystallization and preliminary X-ray analysis of a thermoalkalophilic lipase from *Bacillus stearothermophilus* L1. *Acta Crystallog. sect. D*, **57**, 1300–1302.
29. Harding, M. M. (2001). Geometry of metal–ligand interactions in proteins. *Acta Crystallog. sect. D*, **57**, 401–411.
30. Jaenicke, R. & Boehm, G. (1998). The stability of proteins in extreme environments. *Curr. Opin. Struct. Biol.* **8**, 738–748.

31. Vieille, C. & Zeikus, G. (2001). Hyperthermophilic enzymes: sources, uses, and molecular mechanisms for thermostability. *Microbiol. Mol. Biol. Rev.* **65**, 1–43.
32. Smith, C. A., Toogood, H. S., Baker, H. M., Daniel, R. M. & Baker, E. N. (1999). Calcium-mediated thermostability in the subtilisin superfamily: the crystal structure of Bacillus Ak.1 protease at 1.8 Å resolution. *J. Mol. Biol.* **294**, 1027–1040.
33. Teplyakov, A. V., Gros, P. & Hol, W. G. (1996). Crystallographic study of eglin-C binding to thermitase. *Advan. Expt. Med. Biol.* **379**, 5–9.
34. Fujii, T., Hata, Y., Ooseki, M., Moriyama, H., Wakagi, T., Tanaka, N. & Oshima, T. (1997). The crystal structure of zinc-containing ferredoxin from the termoacidophilic archaeon *Sulfolobus* sp. strain 7. *Biochemistry*, **36**, 1505–1513.
35. Massova, I., Pirkle, H., Edwards, B. F. P. & Mobashery, S. (1997). Insights into the three-dimensional structure of crotalase: implications for biological activity and substrate specificity. *Bioorg. Med. Chem. Lett.* **7**, 3139–3144.
36. Stevens, R. C., Gouaux, J. E. & Lipscomb, W. N. (1990). Structural consequences of effector binding to the T-state of aspartate carbamoyltransferase: crystal structures of the unligated and ATP-complexed and CTP-complexed enzymes at 2.6 Å resolution. *Biochemistry*, **29**, 7691–7701.
37. Otwinowski, Z. & Minor, W. (1997). Processing of X-ray diffraction data collected in oscillation mode. *Methods Enzymol.* **276**, 307–326.
38. Terwilliger, T. C. & Berendzen, J. (1999). Automated MAD and MIR structure solution. *Acta Crystallog. sect. D*, **55**, 849–861.
39. Perrakis, A., Morris, R. & Lamzin, V. S. (1999). Automated protein model building combined with iterative structure refinement. *Nature Struct. Biol.* **6**, 458–463.
40. Hooft, R. W., Vriend, G., Sander, C. & Abola, E. E. (1996). Errors in protein structures. *Nature*, **381**, 272.
41. Esnouf, R. M. (1997). An extensively modified version of MolScript that includes greatly enhanced coloring capabilities. *J. Mol. Graph.* **15**, 132–134.
42. Kabsch, W. & Sander, C. (1983). Dictionary of protein secondary structure: pattern recognition of hydrogen-bonded and geometrical features. *Biopolymers*, **22**, 2577–2637.
43. Kraulis, P. (1991). MOLSCRIPT — a program to produce both detailed and schematic plots of protein structures. *J. Appl. Crystallog.* **24**, 946–950.

***Edited by R. Huber***

*(Received 1 July 2002; received in revised form 8 September 2002; accepted 9 September 2002)*

*Note added in proof*: The crystal structure of a similar thermostable lipase from *B. stearothermophilus* L1 has recently been published (Jeong, S.-T., Kim, H.-K., Kim, S.-J., Chi, S.-W., Pan, J.-G., Oh, T.-K. & Ryu, S.-E. (2002). *J. Biol. Chem.* **277**, 17041–17047).